Multilayer Dielectric Elastomers for Fast, Programmable Actuation without Prestretch

Mihai Duduta, Robert J. Wood, and David R. Clarke*

Dielectric elastomers are a class of versatile transducers that hold great promise for muscle-like soft actuators,[1,2] due to their ability to convert electrical into mechanical energy and vice versa.[3,4] The simplest device consists of a thin elastomer sheet sandwiched between two compliant electrodes. In the actuation mode, a voltage is applied to the electrodes and the attractive Coulombic force between the opposing charges compresses the elastomer causing it to expand in the direction perpendicular to the applied electric field. More complex shape changes can be produced by combining with other passive structures to produce out of plane actuation.[5] The simplest example is a cantilever beam where the dielectric elastomer actuator (DEA) is attached to a passive layer to create a unimorph whose deflection and blocked force are dependent on the applied voltage. Other more complex, voltage controlled shape changes have been demonstrated, such as tunable lenses,[6] soft electroadhesive grippers,[7] and transparent loudspeakers,[8] but the unimorph is a simple actuator that can be used to compare different materials and configurations.

Despite their intrinsic simplicity, DEAs have two major limitations that prevent their wider adoption. The first is the need for prestretching of the elastomer in order to attain large actuation strains.[9] By prestretching, the well-established electromechanical instability is suppressed and higher actuation voltage can be attained before dielectric breakdown occurs.[10] However, prestretching is typically achieved with the use of a rigid frame, which in turn limits the integration of DEAs with other soft components. Some progress has been made to devise elastomer compositions, such as ones consisting of two interpenetrating polymer networks (IPNs).[11] In these network materials, the first elastomer is prestretched, then a second, interpenetrating polymer network is cross-linked throughout the first. When the first elastomer is released, the internal tensile stress is balanced by the compressive stress in the second network, and the elastomer retains some of the prestretch without using a rigid frame. Another approach that has shown some advantages is to manipulate the composition to create a rapid stiffening behavior above a certain stretch value, suppressing the onset of electromechanical instability.[12]

The second major limitation of DEAs is the high voltage typically required for actuation (≈100 V μm^{-1}).[13] Smaller actuation voltages (100–300 V) can be achieved by using much thinner elastomer films (3 μm),[14] but such films are very fragile and difficult to manipulate to create structures. The development of multilayer actuators has improved robustness[15] but as the thickness of the individual layers approaches the thickness of the electrodes, their combined stiffness limits the attainable actuation strains. Decreasing the thickness of the electrodes then becomes necessary but this has proven difficult for silicone actuators because silicones, having low surface energies, adhere poorly to most other materials. Furthermore, good adhesion between the individual electrodes and elastomer layers in the multilayer is necessary to prevent delamination. Hitherto, the most reliable electrodes for silicone based actuators have been physical dispersions of carbon black particles in silicone but these are much stiffer than the silicone itself and invariably have appreciable thickness (>1 μm).[16–18] By comparison, acrylic elastomers are most often good adhesives and can incorporate a wider variety of conductors with minimal increase in stiffness, including conductive powders such as carbon black and silver nanowires.[19,20] As will be shown in this work, certain acrylic compositions can readily incorporate single wall carbon nanotube (SWCNT) mattes so the electrodes can be much thinner and still provide percolative electrical conduction. The acrylic elastomers also have sufficient adhesion between the layers to build mechanically robust multilayer devices.

In this work, we describe a combination of materials and multilayer fabrication method that overcomes these existing limitations, namely the need for prestretch and the high actuation voltage. Moreover, the combination of materials and the method provides the opportunity to create novel actuator structures through the design and placement of the electrodes. These outcomes become possible when, as achieved in this work, the electrode thickness is sufficiently small that the electrodes do not significantly alter the thickness or the stiffness of the elastomer layers. Our approach is to start with an acrylic composition that can be spin cast as a liquid, and then UV cured. The base acrylic composition has already been shown to be capable of actuation without prestretch[12] and several modifications are introduced in this work. The acrylic compositions also have sufficient inherent adhesion that an ultrathin matte of SWCNTs[21] can be transferred directly onto it through a mask to create compliant electrodes. A new elastomer layer can then be spun coat on top, UV cured and the process repeated to create the desired number of multilayers. The step-by-step fabrication process is presented in **Figure 1**a. As shown in this work, the fabrication process can be modified to program complex actuator motions through simple geometric changes in electrode design, something that is not achievable using more traditional methods and materials.

M. Duduta, Prof. R. J. Wood, Prof. D. R. Clarke
John A. Paulson Harvard School of Engineering and Applied Sciences
11 Oxford St., Cambridge, MA 02138, USA
E-mail: mduduta@g.harvard.edu

DOI: 10.1002/adma.201601842

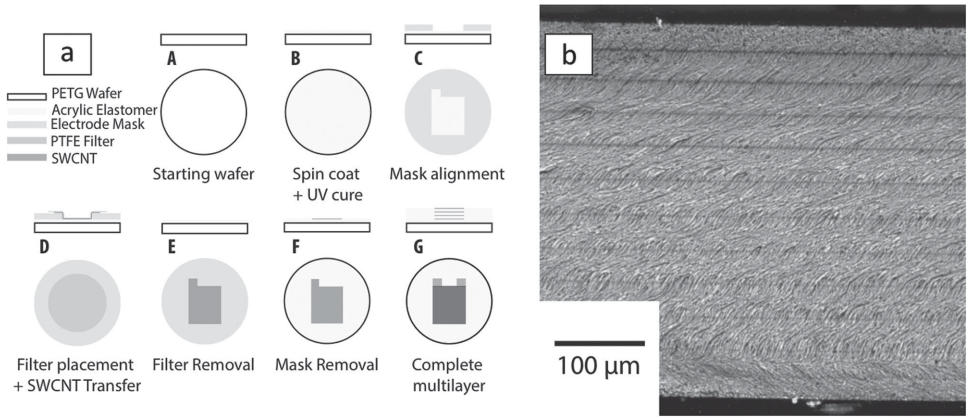

Figure 1. a) Schematic of the assembly process for multilayer dielectric elastomers incorporating SWCNT electrodes. b) Confocal microscopy image of the cross-section of a 12-layer stack made using elastomer B with 10% HDDA cross-linker. The fracture markings obscure some of the electrode layers.

Three different acrylic liquid oligomers were investigated: A (CN9021), B (CN9014), and C (CN9018). The first is the same as previously investigated by Niu et al.,[12] whereas B and C have not previously been used as dielectric elastomers. Each of the oligomers can be cross-linked using 1,6-hexanediol diacrylate (HDDA) and can be UV cured. To demonstrate the viability of this approach, unimorphs have been fabricated by building up the multilayers, then attaching a thin Mylar sheet, which serves as the passive layer. Evaluation of the unimorph characteristics as well as of the elastomers and the adhesive strength of the layers are described in the following section. These include experiments of the unimorph frequency response demonstrating the bandwidth can be controlled by composition. Improvements in actuator bandwidth are necessary for acrylic-based DEAs, to compete with silicone elastomers in terms of actuation response speed.[6,22]

Strong adhesion between the elastomer and electrode layers is an essential requirement for multilayer device fabrication. All the formulations investigated, over a range of 0%–15% by mass of HDDA cross-linker, had sufficient adhesion to completely transfer SWCNT networks at concentrations as high as 22.5 mg m^{-2}. The adhesion strength, quantified using a pull off test, was found decrease slightly with cross-linker concentration (**Figure 2**a). The most adhesive was elastomer A without any cross-linker. For this reason, it was used throughout this work as the base for building multilayers by spin coating on a polyethylene terephthalate glycol (PETG) support wafer. Cross-sections of the multilayers indicated that there was good layer uniformity, as illustrated in the confocal image of Figure 1b, for a 12-layer structure using elastomer A as base and eleven layers of 10% HDDA cross-linked precursor B. In this example the average layer thickness was 37.7 ± 1.6 µm without SWCNT electrodes. The SWCNT electrodes were difficult to discern by confocal imaging making measurements of their thickness unreliable but they were estimated to be <100 nm thick. The presence of the SWCNT electrodes decreased the adhesive strength between the elastomer layers as the concentration of the SWCNT increased (Figure S2, Supporting Information) but no delamination was observed in any of the unimorph tests. Furthermore, the adhesive failure always occurred within the elastomer impregnated SWCNT layer, leaving SWCNT on both of the separated surfaces.

Tensile testing of the elastomers, shown in Figure 2b, indicated that all of them had similar nonlinear strain stiffening behavior. Elastomer B is significantly stiffer than either A or C, while C has higher elongation at failure than A. As expected, the effect of cross-linking is to increase the elastic modulus at the expense of the stretch to failure. More importantly, as shown in Figure 2c, the stress–strain response is nearly identical for a single elastomer layer, compared to a multilayer absent any electrodes and a multilayer with SWCNT electrodes. The data clearly show that the presence of the electrodes in these multilayers neither increases the stiffness of the multilayers nor affects the attainable stretch to failure.

As mentioned earlier, the work of Niu et al. showed that voltage controlled actuation of the elastomer A could be achieved without prestretching. We have found that all three of the elastomers studied also show actuation without prestretching. The results, obtained under biaxial conditions for single layer actuators, are shown in Figure S1c (Supporting Information).

To evaluate the actuation performance of the multilayers in a unimorph configuration, measurements were made of the blocked force, the free-end displacement, and the actuator bandwidth of unimorphs all having the same dimensions (20 mm long and 5 mm wide). The energy density of the actuators was estimated as $\mathbf{FB}\delta/\mathbf{2m}$, where F_B is the blocked force, δ is the displacement, and m is the mass of the actuator. Similarly, the power density was estimated as the product of the energy density and the actuator bandwidth. The three different elastomers with 10% cross-linker were each made into 12 layer unimorphs consisting of individual layers each ≈30 µm thick. At low frequencies, the end displacement was independent of frequency but at higher frequencies, the peak-to-peak end displacement decreased. The frequency at which the peak-to-peak displacement decreased sharply with frequency was identified as the maximum bandwidth of the actuator. Elastomers made with elastomer A had the highest energy density, while B and C had significantly higher bandwidths, and therefore higher power densities (**Table 1**). The specific dependence of displacement

Adv. Mater. **2016**,
DOI: 10.1002/adma.201601842

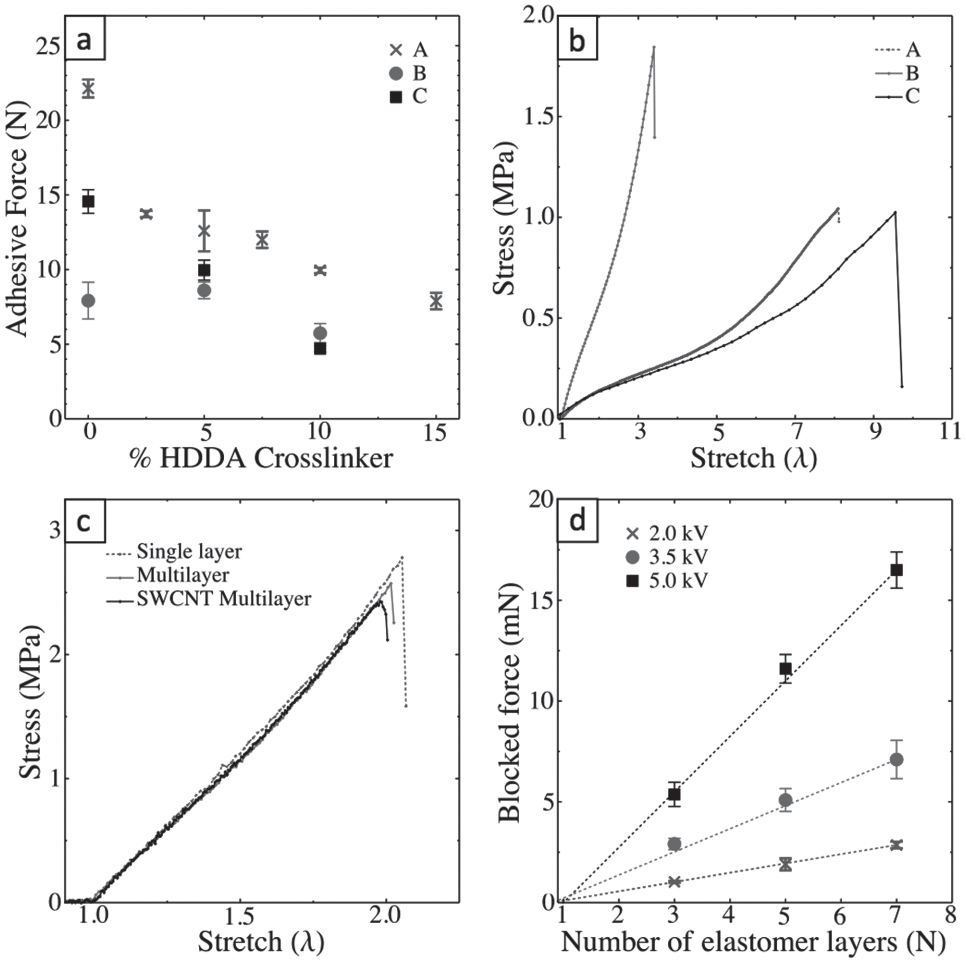

Figure 2. a) Adhesive force required to separate a flat sheet of polytetrafluoroethylene (PTFE) from a pristine layer of elastomer as a function of the type of prepolymer and cross-linker concentration. b) Stress versus stretch curves for different elastomers without any HDDA cross-linker. c) Stress versus stretch curves for elastomer A with 10% cross-linker in three different configurations: single layer, six-layer multilayer, and six-layer multilayer with SWCNT embedded electrodes. The thickness of each test sample was the same (≈90 μm). d) Blocked force as a function of number of elastomer layers of equal thickness (70 μm layers, elastomer A with 10% HDDA) at the three different voltages indicated.

on actuation frequency is shown in **Figure 3**b. From measurements of the electrical current during actuation, the time to charge each of the multilayers was found to be similar, being in the 1–10 ms range, suggesting that the bandwidth differences were due to different viscoelastic responses of the elastomers rather than being an electrical time constant for the RC circuit containing a resistor (R) and a capacitor (C). In addition, measurements of blocked force in three, five, and seven-layer unimorph actuators showed a linear dependence of the force on the number of layers in the device (Figure 2d), consistent with simple mechanics models.

The multilayer fabrication method was effective at lowering the actuation voltage. For example, a unimorph made with 25 μm single layers deformed significantly with voltages of 1–2 kV (Figure 3a), a value at the low range of actuation voltages reported thus far.[10] Occasionally, it was found that even lower actuation voltages (≈600 V) could be obtained with thinner elastomers but this was not reproducible because of the

Table 1. Unimorph performance for devices built from 12 layers of elastomer of 40 μm each. The unimorph width was 5 mm and the length was 20 mm, weighing ≈50 mg, while the actuation voltage was 4 kV. Three actuators were tested for each precursor type, all tests were performed five times. The fastest actuator in each configuration was used to determine the resonant frequency.

Precursor type	Blocked force [mN]	Maximum displacement [mm]	Maximum bandwidth [Hz]	Energy density [J kg^{-1}]	Maximum power density [W kg^{-1}]
A	16.9 ± 1.0	12.0 ± 0.3	1	2.04 ± 0.12	2.04 ± 0.12
B	12.5 ± 0.9	15.6 ± 0.4	10	1.95 ± 0.10	19.5 ± 1.01
C	11.1 ± 0.6	12.6 ± 0.4	30	1.42 ± 0.08	42.6 ± 2.42

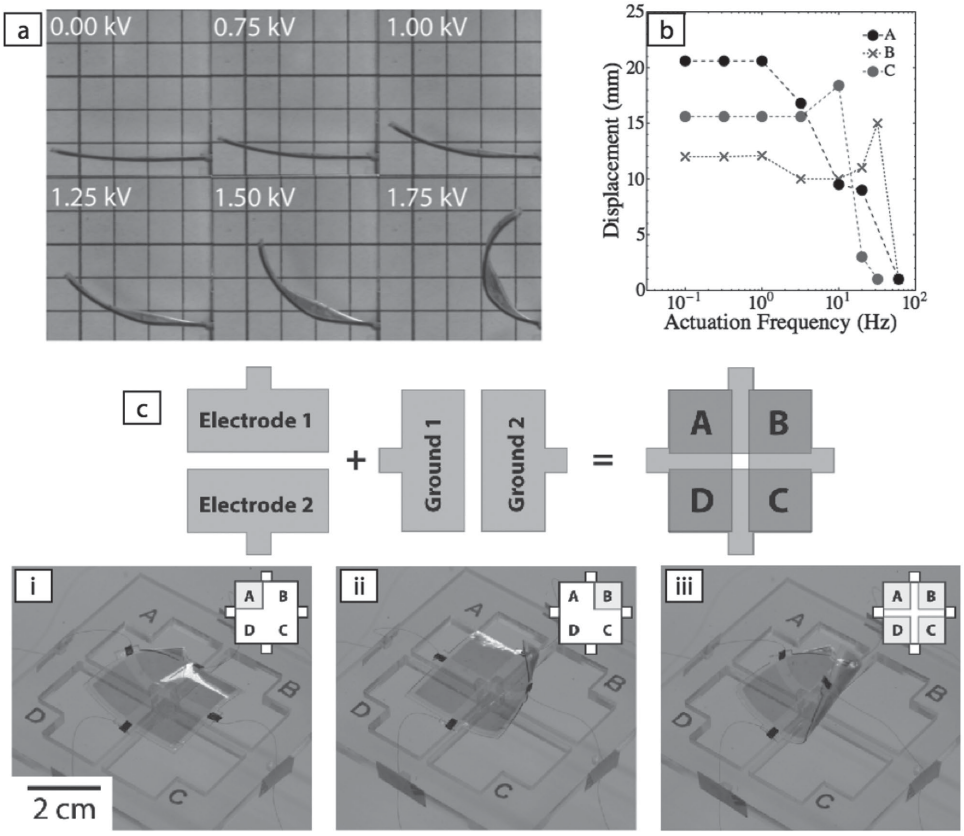

Figure 3. a) Images of a 12-layer elastomer A with 10% HDDA in a unimorph configuration at six different applied voltages. The grid spacing in the background is 5 mm. b) End displacement of the unimorph as a function of frequency actuated at 4 kV. c) Schematic of electrode patterns used to make a simple 2 × 2 multimorph actuator. (i) Photograph of an eight layer, elastomer A with 10% HDDA multilayer unimorph with voltage applied to segment A, (ii) voltage applied to segment B, and (iii) voltage applied to all segments. Actuation voltages are 3.75 kV.

unavoidable presence, at least in our experiments, of air borne particulates. Indeed, the total number of layers will be limited by the process tolerance to prevent defects in the elastomer, since dielectric breakdown in any one layer can lead to breakdown of the multilayer device through an electrical short.

The fabrication method also enabled us to devise more complex, and programmable, actuation actions into a single device. This is illustrated in Figure 3c where, by varying the pattern of electrodes between different layers, we created a multimorph actuator capable of nine different deformation modes when different electrodes were powered. The multiple degrees of freedom were built in by controlling the geometries and electrical connection paths of each of the four electrodes. Three actuation modes are shown in Figure 3c, while the full capabilities are captured on video and presented in the Supporting Information. While the multimorph presented is quite basic, the principle behind it can be used to create much more complex motion, beyond traditional DEA architectures.

We have demonstrated that the performance of DEAs (maximum strain, energy density, and actuator bandwidth) can be tuned by controlling both the choice of elastomer precursor and the cross-linker concentration. The cross-linking concentration increased the stiffness, reduced the maximum elongation before failure, and decreased the adhesive strength of the elastomers. The Young's modulus for elastomer B without any HDDA cross-linker (0.66 MPa) was almost an order or magnitude higher than elastomer A (0.1 MPa). Meanwhile, precursor C had similar stiffness, but slightly larger extension range, without being as adhesive. Between the three precursors and the ability to vary cross-linker density, the range of mechanical properties for acrylic elastomers that actuate without prestretch is greatly expanded. The unimorph actuator testing revealed that the novel oligomers, elastomers B and C, offered additional advantages over previous compositions. The increase in resonant frequency from 1 (for A) to 30 Hz (for B) confirmed that tailoring the material composition could overcome some of the known drawbacks of acrylic elastomers such as slow actuation speed.[23] The energy densities were comparable to other multilayer geometries,[15] but the power densities reported here broaden the range of potential applications.

The combination of liquid acrylic oligomers, UV curing, and the intrinsic adhesiveness of the acrylics together with standard spin coating, patterning, and dry transfer of SWCNT by stamping enables the fabrication of multilayer dielectric elastomer devices. This is exemplified in this work by the fabrication of multilayer unimorphs. The significance of this work is that the combination of materials and processing enables two of the current technical limitations of DEAs to be overcome. Specifically, the compositions studied remove the requirement that the elastomer has to be prestretched. The use of a liquid

DOI: 10.1002/adma.201601842

precursor that can be UV cured after each layer enables thinner elastomer layers to be obtained, decreasing the voltage required for actuation. The thickness of the individual layers can be determined by control of the spin coating process and the viscosity of the liquid. Thinner SWCNT electrodes decrease the effective electrode stiffness that, in turn, increases the attainable actuation strain for a given applied voltage. The natural adhesion of the acrylics increases the reliability of the stamping of the SWCNT as well as adhesion to a wider range of substrate materials. Furthermore, the ability to create the electrodes by stamping (or spraying) facilitates patterning of the electrode geometries, including doing so at different positions in the multilayer structure. Unimorphs fabricated exhibit similar blocked forces and energy densities as have been reported but at lower actuation voltages. A simple 2D actuator is demonstrated illustrating the potential of electrode patterning. Overall the process can be tuned to fabricate versatile devices, in which the number, thickness, planar geometry, electrode coupling, and chemical nature of the layers can be manipulated to design actuators for specific applications. The multimorph actuator highlights a novel approach to creating smart programmable materials capable of multiple degrees of freedom from limited inputs. Beyond improving DEAs, we consider the combination of acrylic elastomers and stretchable carbon nanotube network electrodes to be a materials platform technology, applicable to other areas, such as stretchable sensors, soft sensor-actuator combinations, soft electroadhesives to name a few.

Experimental Section

The elastomer oligomers used (CN9021, CN9014, and CN9018) were obtained from Sartomer Company (Exton, PA) and the cross-linker HDDA was procured from Sigma-Aldrich (St. Louis, MO). The detailed compositions are reported in the Supporting Information. Evaluation of the mechanical and electrical properties of the elastomer and electrodes was based on standards from the American Society for Testing and Materials (ASTM) or current DEA standards.[24] The CN9021 oligomer (A) was the basis for the composition reported by Niu et al.,[12] while CN9014 (B) and CN9018 (C) are being presented for the first time. A schematic of the multilayer assembly process is depicted in Figure 1c. The multilayer devices were made through consecutive elastomer spin coating, UV curing, and electrode transfer steps. The oligomers were spun coated onto PETG-modified substrates in a Model WS-650MZ-23NPP/LITE spin coater from Laurell Technologies Corporation (Figure 1c, steps A, B). UV curing was performed in an Ever Bright Printing Machine Fty. Ltd that has a peak output at 365 nm. The electrode mask was laser cut from Mylar silicone-coated to minimize adhesion to the elastomers (step C). The SWCNT were directly transferred onto the UV cured acrylic elastomers through the mask (steps D, E, F). The spin coat, cure, and electrode transfer process were repeated to produce the desired number of layers (an example four layer device is shown in step G). The devices were laser cut (Versalaser, CO_2 60 W) from the multilayer stack. The electrode size was limited by the size of available PTFE filters used to transfer the SWCNTs. Multiple filters were used to make electrodes with features larger than the dry SWCNT matte diameter of 30 mm.

The unimorph actuators, fabricated by depositing the multilayers on a stiff sheet of Mylar (12.5 μm thick) in a cantilever configuration: 20 mm long and 5 mm wide. The thickness was 0.05–1 mm, depending on the number of layers coated and the spin coating conditions. Mylar was selected as it has a relatively large Young's modulus (1 GPa) and little thickness variability. The actuation power source was a TREK Model 610E. The blocked force was measured with a Futek 50 g load cell in contact with the free end of the unimorph actuator. Similarly, images of flexural displacement of the end of the unimorph were recorded as a function of applied voltage. The end displacements were determined from photos or videos (180 frames s^{-1}) using ImageJ software. The actuation bandwidth was determined by applying an alternating current from a Wavetek 75 Arbitrary Waveform Generator and measuring the peak-to-peak time-averaged displacement. A multimorph actuator was made as shown in Figure 3b: the power electrode was separated into two segments, as was the ground electrode. By rotating the power electrodes by 90° relative to the ground electrodes it was possible to create four zones that could be actuated independently.

Supporting Information

Supporting Information is available from the Wiley Online Library or from the author.

Acknowledgements

The authors gratefully acknowledge funding from the National Science Foundation (Grant No. DMR14-20570), Wyss Institute for Biologically Inspired Engineering, and the Link Foundation Fellowship. Any opinions, findings, and conclusions or recommendations expressed in this material are those of the authors and do not necessarily reflect the views of the National Science Foundation.

Received: April 6, 2016
Revised: May 31, 2016
Published online:

[1] S. Kim, C. Laschi, B. Trimmer, *Trends Biotechnol.* **2013**, *31*, 5.
[2] D. Trivedi, C. D. Rahn, W. M. Kier, I. D. Walker, *Appl. Bionics Biomech.* **2008**, *5*, 3.
[3] R. Pelrine, R. Kornbluh, Q. Pei, J. Joseph, *Science* **2000**, *287*, 5454.
[4] R. Pelrine, R. Kornbluh, G. Kofod, *Adv. Mater.* **2000**, *12*, 16.
[5] S. Shian, K. Bertoldi, D. R. Clarke, *Adv. Mater.* **2015**, *27*, 43.
[6] F. Carpi, G. Frediani, S. Turco, D. De Rossi, *Adv. Funct. Mater.* **2011**, *21*, 21.
[7] J. Shintake, S. Rosset, B. Schubert, D. Floreano, H. Shea, *Adv. Mater.* **2016**, *28*, 2.
[8] C. Keplinger, J. Y. Sun, C. C. Foo, P. Rothemund, G. W. Whitesides, Z. Suo, *Science* **2013**, *341*, 6149.
[9] G. Kofod, *J. Phys. D: Appl. Phys.* **2008**, *41*, 21.
[10] X. Zhao, Z. Suo, *Phys. Rev. Lett.* **2010**, *104*, 17.
[11] S. H. Ha, W. Yuan, Q. Pei, R. Pelrine, S. Stanford, *Adv. Mater.* **2006**, *18*, 7.
[12] X. Niu, H. Stoyanov, W. Hu, R. Leo, P. Brochu, Q. Pei, *J. Polym. Sci., Part B: Polym. Phys.* **2013**, *51*, 3.
[13] J. S. Plante, S. Dubowsky, *Int. J. Solids Struct.* **2006**, *43*, 25.
[14] A. Poulin, S. Rosset, H. Shea, *Appl. Phys. Lett.* **2015**, *107*, 24.
[15] G. Kovacs, L Düring, S. Michel, G. Terrasi, *Sens. Actuators, A* **2009**, *155*, 2.
[16] S. Rosset, H. Shea, *Appl. Phys. A* **2013**, *110*, 2.
[17] O. A. Araromi, A. T. Conn, C. S. Ling, J. M. Rossiter, R. Vaidyanathan, S. C. Burgess, *Sens. Actuators, A* **2011**, *167*, 2.
[18] P. Lotz, M. Matysek, H. F. Schlaak, *IEEE/ASME Transactions on Mechatronics* **2011**, *16*, 1.

[19] W. Yuan, L. B. Hu, Z. B. Yu, T. Lam, J. Biggs, S. M. Ha, D. J. Xi, B. Chen, M. K. Senesky, G. Grüner, Q. Pei, *Adv. Mater.* **2008**, *20*, 3.
[20] S. Shian, R. M. Diebold, A. McNamara, D. R. Clarke, *Appl. Phys. Lett.* **2012**, *101*, 6.
[21] S. Shian, R. M. Diebold, D. R. Clarke, *Opt. Express* **2013**, *21*, 7.
[22] L. Maffi, S. Rosset, M. Ghilardi, F. Carpi, H. Shea, *Adv. Funct. Mater.* **2015**, *25*, 11.
[23] I. A. Anderson, T. Hale, T. Gisby, T. Inamura, T. McKay, B. O'Brien, S. Walbran, E. Calius, *Appl. Phys. A* **2010**, *98*, 1.
[24] F. Carpi, I. A. Anderson, S. Bauer, G. Frediani, G. Gallone, M. Gei, C. Graaf, C. Jean-Mistral, W. Kaal, G. Kofod, M. Kollosche, *Smart Mater. Struct.* **2015**, *24*, 10.

Adv. Mater. **2016**,
DOI: 10.1002/adma.201601842